RSC Sustainability

ROYAL SOCIETY OF CHEMISTRY

PAPER

View Article Online
View Journal | View Issue

Cite this: *RSC Sustainability*, 2023, **1**, 2058

Vacuum pyrolysis depolymerization of waste polystyrene foam into high-purity styrene using a spirit lamp flame for convenient chemical recycling†

Eri Yoshida *

Waste plastic pollution is a pressing global issue. In particular, waste polystyrene (PS) foam causes significant damage to marine ecosystems due to its toxic decomposition products. However, effective recycling methods for waste PS foam have not yet been developed. With the aim of establishing an efficient chemical recycling process for waste PS, this study presents a simple and convenient method for recovering high-purity styrene from waste PS foam by vacuum pyrolysis depolymerization. The vacuum pyrolysis of waste PS foam was performed in a Pyrex tube, ignited using a spirit lamp flame for 20 min, resulting in a recovery of 98%-purity styrene in a 55% yield. The yield was further increased to 67% by conducting the pyrolysis in the presence of molecular sieves, which prevented side reactions such as backbiting and radical coupling. Additionally, increasing the temperature enhanced the styrene yield. This vacuum pyrolysis depolymerization process for chemical recycling requires no temperature controller or monomer fractionation. It can be applied to various waste plastics with carbon–carbon backbones, thus offering a promising solution for reducing plastic waste. Furthermore, the closed loop system, which includes monomer recovery without the need for purification and its reuse for reproducing the original products, also contributes to a reduction in natural fossil fuel consumption.

Received 25th June 2023
Accepted 26th September 2023

DOI: 10.1039/d3su00207a

rsc.li/rscsus

Sustainability spotlight

To address the intensifying plastic waste, it is crucial to establish closed-loop recycling systems that involve recovering component monomers from waste plastics and utilizing the monomers to reproduce the original products. This approach not only reduces waste plastics but also minimizes the consumption of natural fossil fuels by reusing fossil fuel-based monomers. However, chemical recycling of waste plastics into compounds different from the component monomers forms an open-loop recycle while recycling into impure monomers diminishes the performance of the reproduced products. This study presents a vacuum pyrolysis depolymerization method utilizing a spirit lamp flame, which effectively achieves high-purity styrene recovery from waste polystyrene foam, thereby preserving the original performance of the reproduced products. This simple pyrolysis method can be applied to all types of non-biodegradable waste plastics with carbon–carbon backbones, thus promising sustainable industrial development and fostering global economic growth. This study emphasizes its consistency with the United Nations' Sustainable Development Goals (SDGs), particularly SDG 12 (sustainable consumption and production), SDG 7 (affordable clean energy) and SDG 14 (life below water).

Introduction

Waste plastic pollution has been a significant concern for over 40 years. During this period, the accumulation of waste plastics has continued to increase and is now approaching 8 billion tons with an annual production of 400 million tons.[1–3] If no measures are taken to address this issue, it is projected that waste plastics will double within the next 20 years, reaching 33 billion tons by 2050.[4,5] While various bio-based and biodegradable polymers have been developed as alternatives to non-biodegradable plastics,[6–9] a significant amount of non-biodegradable waste plastics persists, accumulating on land and in the oceans without decomposing. The primary culprits behind plastic pollution are petrochemical-based polymers with a carbon–carbon backbone, mainly polyethylene, polypropylene, polyvinyl chloride and polystyrene (PS).[3,10] The plastics left outdoors undergo fragmentation through weathering and exposure to sunlight[11] into microplastics, which cause health damage and disrupt ecosystems through the food chain.[12–14] Of particular concern are PS microplastics, which account for 16% of the total microplastics.[15] These microplastics cause severe harm to marine organisms due to the generation of toxic aromatic-based decomposition products.[16–18]

Department of Applied Chemistry and Life Science, Toyohashi University of Technology, 1-1 Hibarigaoka, Tempaku-cho, Toyohashi 441-8580, Japan. E-mail: yoshida.eri.gu@tut.jp

† Electronic supplementary information (ESI) available. See DOI: https://doi.org/10.1039/d3su00207a

Polystyrene, accounting for 6% of primary plastic waste generation in 2015,[3] has diverse applications such as containers, electrical and heat insulators, building materials and protective packaging due to its easy moldability, structural stability, chemical resistance and mechanical strength. The lightweight nature of PS foam, with a density of 0.016–0.64 g cm^{-3} (lower than other carbon–carbon backbone plastics ranging from 0.90 to 1.45 g cm^{-3}) based on its 98% air content,[18,19] makes it widely used as a material for food containers. However, the disposal of waste PS foam poses a significant environmental challenge. The foam can contribute to pollution in rivers and oceans as it remains buoyant on the surface.[20] The fragmentation into microplastics is facilitated in the floating foam by absorbing UV rays with the phenyl groups of the PS.[21]

Some methods have been developed for the recycling of waste plastics. Mechanical recycling, which involves reusing plastics without chemical modification,[22] such as in wood composites[23] and cement composites,[24] is an easy way to reuse plastics. However, mechanical recycling does not reduce the amount of waste plastics. Enzymatic recycling, which relies on decomposition by bacteria, is an environmentally friendly method. However, it is currently limited to only a few types of plastics, such as poly(ethylene terephthalate) and polyurethane, among the petrochemical-based polymers, and cannot be applied to PS.[25] Recycling methods using bio-derived Ni catalysts under microwave irradiation have been developed,[26,27] which can degrade polyethylene into hydrocarbons and hydrogen and also assist in the depolymerization of PS into styrene. In recent years, several chemical recycling methods have been developed for PS, particularly waste PS foam. These methods include oxidation into carboxylic acids and ketones,[28–30] post-polymerization modification[31] and gasification for syngas fuel production.[32,33]

Pyrolysis typically requires high temperatures above 300 °C;[34,35] however, it is a well-studied approach due to its numerous advantages, including the absence of solvents.[36,37] Nevertheless, certain pyrolysis studies cannot be directly applied to the chemical recycling of waste PS foam due to the requirement of additional reactors and the need to fractionate the resulting monomers. Thermogravimetric analysis methods have proven efficient in depolymerizing PS into styrene through pyrolysis at temperatures above 400 °C,[38,39] however, the methods are not practical for recovering the monomer. Pyrolysis using (semi-)batch reactors,[40–45] fixed bed reactors[46,47] or microwaves as a heat source[48] recovered styrene, but the resulting styrene often contains other aromatic hydrocarbons like toluene, ethylbenzene and isopropylbenzene. These hydrocarbons act as chain transfer agents during the radical polymerization of styrene, leading to a decrease in the molecular weight of PS and a subsequent reduction in the mechanical strength of the resulting products.[40,49] Moreover, aromatic decomposition products, such as pyrene, phenanthrene and polycyclic compounds, pose potential carcinogenic risks.[50,51] Therefore, it is crucial to recover the high purity of styrene in order to incorporate the monomer recovery and PS reproduction processes in the closed-loop recycling system in a safe manner.

This paper describes vacuum pyrolysis using a spirit lamp flame for the effective depolymerization of waste PS foam, resulting in the recovery of styrene with a 98% purity in just 20 min. This simple and convenient chemical recycling method, which involves heating the waste plastics in a Pyrex tube with suction and not requiring a specific reactor or temperature controller, could be widely applicable to other plastics, leading to reducing waste plastic pollution.

Experimental

Materials

Waste PS foam (Karux Ltd.), provided as a cooling container, was used in this study. Copper, iron and silica gel (Wakogel® C-300, 45–75 μm) were purchased from Fujifilm Wako Pure Chemical Corporation. Molecular sieves of MS-3A (0.3 nm pore size), MS-4A (0.4 nm), MS-5A (0.5 nm) and MS-13X (1 nm) were also purchased from Fujifilm Wako Pure Chemical Corporation. They were all cylindrical with dimensions of 1.6 mm in diameter and 2–6 mm in length. A mixed alcohol fuel (76.6% methanol, 21.4% ethanol and 0.3% isopropanol) for a spirit lamp was purchased from Kenei Pharmaceutical Inc. 2,2′-Azobis(isobutyronitrile) (AIBN) purchased from Fujifilm Wako Pure Chemical Corporation was recrystallized from methanol. Ethylene glycol diethyl ether, with a purity exceeding 98%, was purchased from Tokyo Chemical Industry and used as received. Methanol was purified by distillation over magnesium, with the addition of a small amount of iodine.

Characterizations

Gas chromatography (GC) was performed using a Shimadzu GC-8A gas chromatograph equipped with a thermal conductivity detector and a C-R6A Chromatopac recorder. GC was conducted with helium as the carrier gas using a Shimadzu OV-3 column (3 meters). The injection temperature was set at 90 °C, while the column and final temperatures were both set at 60 °C. ^{1}H NMR and ^{13}C NMR measurements were conducted using Jeol ECS400 and ECS500 FT NMR spectrometers. The molecular weight (M_n) and polydispersity index (PDI = M_w/M_n) of the PS foam and decomposition products were calculated by gel permeation chromatography (GPC) based on PS standards. GPC was performed using a Tosoh GPC-8020 instrument equipped with a DP-8020 dual pump, a CO-8020 column oven and an RI-8020 refractometer. Three PS gel columns of Tosoh TSKGEL G2000H_{XL}, G4000H_{XL} and G6000H_{XL} were used with tetrahydrofuran as the eluent at 40 °C. Time-of-flight mass (TOF-MS) analysis was performed in positive polarity atmospheric pressure chemical ionization (APCI) using a Bruker micrOTOF II-TTUH mass spectrometer with methanol as the eluent. The pyrolysis was carried out under suction using a Sato Vac TST-20 oil rotary vacuum pump. The temperature inside an empty Pyrex tube was measured above the spirit lamp flame under atmospheric pressure using a Toyo Netsu Kagaku TM-710 digital thermometer connected with an R-type thermocouple.

Vacuum pyrolysis of the waste PS foam, general procedure

The vacuum pyrolysis was performed in a Pyrex tube connected to a trap cooled with liquid nitrogen by flaming it with a spirit lamp (Fig. 1). The waste PS foam (305 mg) was placed in a 100 mL Pyrex test tube and heated for 20 min under suction using a vacuum pump and a spirit lamp flame. The trap was purged with argon and left to return to room temperature. The residue in the tube was dissolved in 1,4-dioxane (10 mL) and freeze-dried *in vacuo* using liquid nitrogen. To determine the yield of styrene, ethylene glycol diethyl ether (100 μL) as the standard and methanol (3 mL) were added to the liquid in the trap, and the mixture was subjected to GC analysis.

Characterization of the cyclic trimer

The residue (44 mg) in the tube by the vacuum pyrolysis with copper at a 1.0 weight ratio was subjected to flash column chromatography using cyclohexane as the eluent to isolate a low molecular weight decomposition product. The isolated product was then dried *in vacuo* for several hours to obtain a liquid product (28 mg). The structure of the product was determined by ^{1}H NMR, ^{13}C NMR and TOF-MS. ^{1}H NMR: δ_H (500 MHz, $CDCl_3$, $CHCl_3$, ppm) = 1.84–1.92 (1H, m, CH), 2.01–2.08 (1H, m, CH), 2.32–2.45 (2H, m, CH), 2.60–2.72 (1H, m, CH), 2.78–2.87 (2H, m, CH_2), 4.89 (1H, d, J 1.20, CH_{cis}=), 5.16 (1H, d, J 1.20, CH_{trans}=), 7.03–7.23 (15H, m, Ph). ^{13}C NMR: δ_C (500 MHz, $CDCl_3$, ppm) = 33.75, 37.40, 43.49, 43.72, 114.54, 125.69, 126.21, 126.48, 127.41, 127.83, 128.30, 128.38, 128.41, 141.18, 142.50, 145.08, 146.80. m/z = 337 (M + 1), 369 (M + 1 + CH_3OH).

Radical polymerization of styrene, general procedure

Styrene (1.0 g, 9.60 mmol) and AIBN (47.4 mg, 0.289 mmol) were placed in an ampoule. The contents were degassed using a freeze–pump–thaw cycle three times and purged with nitrogen. The bulk polymerization was carried out at 60 °C for 7 h. The product was dissolved in 1,4-dioxane (10 mL). A portion of the solution was withdrawn to determine the monomer conversion by ^{1}H NMR. The remaining solution was poured into methanol (500 mL) to precipitate PS. The precipitate was collected by filtration, dried, and then subjected to GPC analysis.

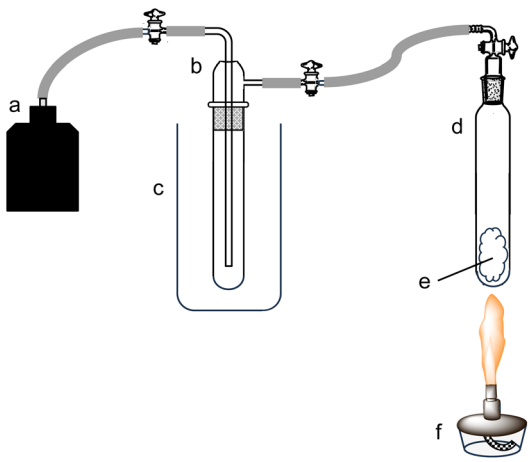

Fig. 1 Vacuum pyrolysis using a spirit lamp flame for styrene recovery from waste PS foam: (a) a vacuum pump, (b) trap to collect styrene, (c) Dewar bottle filled with liquid nitrogen, (d) Pyrex tube, (e) waste PS foam and (f) spirit lamp.

Results and discussion

Characterization of decomposition products

Vacuum pyrolysis was performed on waste PS foam (99% purity by ^{1}H NMR, M_n = 99 900 and M_w/M_n = 2.76 by GPC) in a Pyrex tube by heating using a spirit lamp. The temperature and pressure inside the tube were 420 °C and 1 mmHg, respectively. The waste PS foam melted within a few minutes above the flame and produced a liquid in a 55% yield after 20 min of pyrolysis. The liquid was identified as styrene with a purity of 97.8% as determined by GC and 98.8% by ^{1}H NMR (Fig. 2). TOF-MS confirmed the presence of styrene, as evidenced by m/z = 105 (M + 1) (ESI Fig. S1†). Based on ^{1}H NMR, the styrene contained 1.2% toluene but neither ethylbenzene nor isopropylbenzene. These compounds have chain transfer constants of 5.36 times and 6.56 times greater than toluene, respectively, during styrene polymerization.[52] α-Methylstyrene, which undergoes depolymerization at 61 °C,[52] was not detected during the pyrolysis. The styrene recovered by the pyrolysis produced PS with an M_n of 22 300 and 84% conversion by the radical polymerization with AIBN at 60 °C under N_2 for 7 h. A comparison to pure styrene, which produced PS with an M_n of 27 900 and 96% conversion under identical conditions, further supported the recovery of high-purity styrene (Fig. S2†). The high-purity monomer recovery is attributed to vacuum pyrolysis, in which the polymerization–depolymerization equilibrium is shifted to the depolymerization side by removing the resulting monomer from the reaction system (Fig. 3).

The variation in the styrene yield with time during the pyrolysis is shown in Fig. 4. The styrene yield reached a plateau after 10 min due to the transformation of the PS foam into a viscous liquid. The total yield of the decomposition products slightly decreased within 5 minutes. This suggests that gaseous products, due to their low boiling points under reduced pressure, were not trapped. Not capturing these gaseous products assists in achieving high-purity styrene recovery. Additionally, 1–2% toluene was

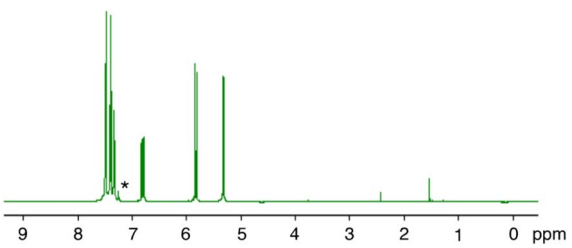

Fig. 2 ^{1}H NMR spectrum of the styrene recovered by the pyrolysis of the waste PS foam. Solvent: $CDCl_3$. * $CHCl_3$.

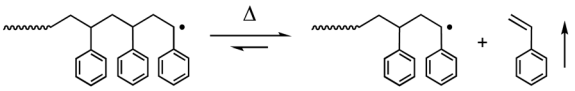

Fig. 3 Enhanced depolymerization process by monomer abstraction during the vacuum pyrolysis.

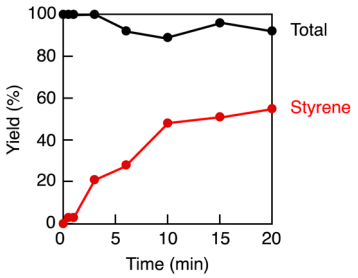

Fig. 4 Variations in the styrene and total yields with time.

consistently detected throughout the pyrolysis, independent of the styrene yield. As the pyrolysis progressed, the residue in the tube underwent a reduction in molecular weight. Fig. 5 displays the ^{1}H NMR spectra of the residue at different pyrolysis times. The signal intensity of the main chain protons in the range of 1.2–2.4 ppm decreased over time due to the degradation. Conversely, the signal intensity of the vinylidene protons at 4.89 and 5.16 ppm increased, indicating the production of olefin compounds during the pyrolysis. The variations in molecular weight and PDI of the waste PS foam during the pyrolysis are shown in Fig. 6. The pyrolysis immediately decreased the molecular weight of PS, suggesting random scission of the main chain followed by depolymerization. This random scission depolymerization, rather than step-by-step depolymerization from the polymer chain

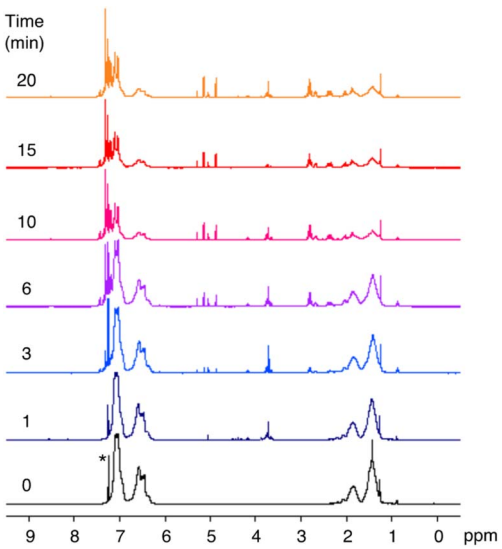

Fig. 5 ^{1}H NMR spectra of the residue in the Pyrex tube for each time. Solvent: $CDCl_3$. * $CHCl_3$.

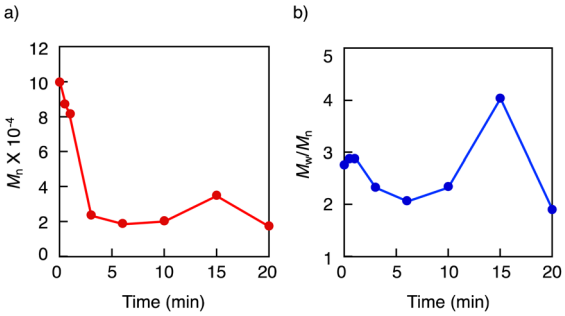

Fig. 6 Plots of (a) the molecular weight (M_n) and (b) PDI (M_w/M_n) of the residue *versus* time.

end, was supported by the degree of decrease in the molecular weight for a given styrene yield. For example, at a 21% styrene yield after 3 min of pyrolysis, the molecular weight decreased from M_n = 99 900 to 23 700. In the case of step-by-step depolymerization from the polymer chain end, the molecular weight would be calculated to be 78 900 for a 21% decrease. Despite the decrease in molecular weight, the PDI slightly increased during the very initial pyrolysis of 30 s or 1 min, further supporting the random scission mechanism. The pyrolysis process for more than 1 min rapidly reduced both the molecular weight and PDI. However, at 10 min, the molecular weight and PDI increased and reached a maximum of 15 min due to the coupling of the chain end radicals, which often occurs during styrene polymerization and leads to a doubling of the molecular weight. After 15 min, the molecular weight and PDI decreased again as a result of additional pyrolysis.

The variation in the GPC curve of the residue is depicted in Fig. 7. The presence of a bimodal curve during the 15 min pyrolysis supports the occurrence of radical coupling between the polymer chains. The PS curve gradually shifted towards the lower molecular weights, accompanied by a decrease in intensity as the pyrolysis progressed. In contrast, a decomposition product with a molecular weight of approximately M_n = 300 showed an increase in intensity at a retention time of 29 min as the pyrolysis advanced. Fig. 8 displays the GPC area ratios of the respective products obtained during pyrolysis. The area is proportional to the number of molecules with a given molecular weight. Therefore, the area ratio can be considered as the molar ratio of the products. The M_n-300 product exhibited a distinct increase through the main chain degradation unlike other decomposition products. The ^{1}H and ^{13}C NMR, as well as TOF-MS analysis, revealed that this specific product was a 5-membered ring trimer (Fig. 9), which was formed by backbiting (Fig. 10). The formation of this cyclic trimer hindered the generation of styrene.

Additive effect

This study investigated the effect of additives on the pyrolysis to suppress backbiting. The results of the pyrolysis by heating for 20 min are summarized in Table 1. Copper exhibits potential to suppress the backbiting by donating an electron

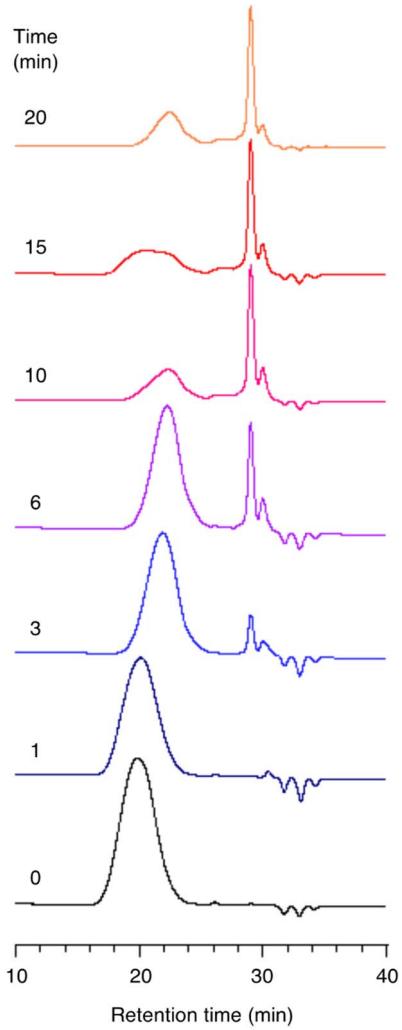

Fig. 7 GPC profiles of the residue for each time.

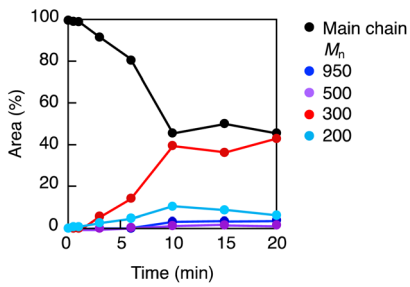

Fig. 8 Variations in area ratios of the decomposition products with time.

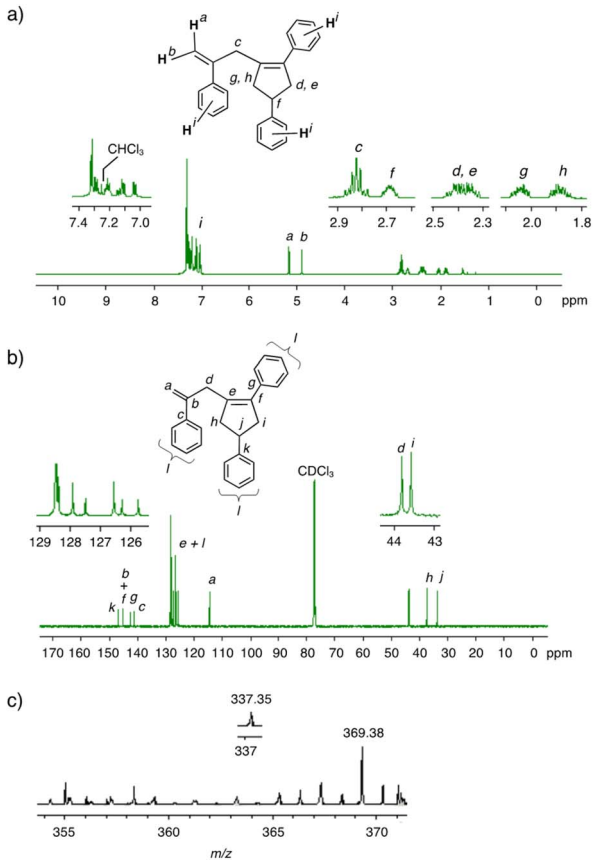

Fig. 9 Characterization of the M_n-300 product; (a) ^{1}H NMR spectrum (solvent: $CDCl_3$), (b) ^{13}C NMR spectrum and (c) mass spectrum. TOF-MS with the APCI method, eluent: methanol.

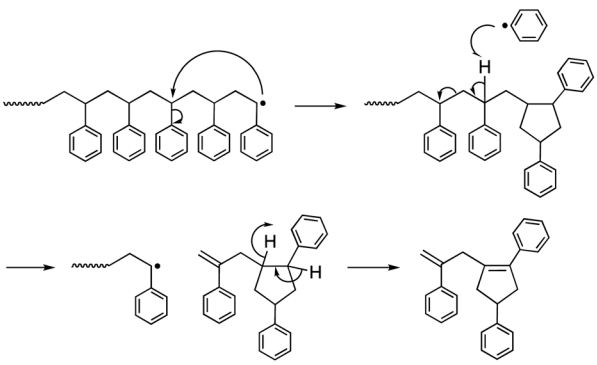

Fig. 10 Mechanism of the backbiting that forms the cyclic trimer.

to the polymer radical to convert it into its anion. Powdery copper at a weight ratio of 0.2 to the PS foam slightly increased the styrene yield, while drastically reducing the cyclic trimer formation by retarding the polymer degradation. The interaction between the polymer radical and its anion suppressed the backbiting. Increasing the copper ratio to 1.0 accelerated the polymer degradation; however, it also enhanced the formation of the trimer along with a decomposition product having a still lower molecular weight of M_n = *ca.* 200. The presence of the polymer anions advanced the backbiting in the absence of the polymer radicals due to the inhibition of anionic depolymerization. Iron has a slightly lower work function (4.50 eV) compared to copper (4.65 eV).[53] Iron powder produced no difference from the copper regarding the styrene yield, however, it increased the PDI of the decomposed polymer. The marked increase in the PDI

Table 1 Effect of the additives on the vacuum pyrolysis depolymerization of the waste PS foam

					Area ratio (%)					
						M_n				
Additive	Weight ratio	St (%)	M_n	M_w/M_n	Polymer	950	500	300	200	Toluene (%)
—	—	55	17 500	1.90	45.5	3.9	1.5	43.0	6.1	2.2
Cu	0.2	58	18 300	1.92	63.3	4.5	1.6	26.1	4.5	1.9
Cu	1.0	59	17 500	1.59	10.0	7.6	2.7	62.0	17.7	2.1
Fe	1.0	58	21 900	3.04	60.5	5.1	2.5	26.1	5.8	2.4
Silica	1.5	55	8390	1.44	10.3	3.1	2.0	54.3	30.3	1.9
MS-3A	1.5	58	18 100	2.07	35.1	4.5	2.9	44.6	12.9	1.1
MS-4A	1.5	66	17 900	2.15	24.1	4.2	2.5	46.4	22.8	6.0
MS-5A	1.5	55	15 900	1.70	11.6	8.0	5.6	50.1	24.7	4.3
MS-13X	1.5	59	15 300	1.86	24.3	5.4	2.2	53.7	14.4	12.7

and increased molecular weight imply that the radical coupling replaced the backbiting. To prevent radical coupling and backbiting by restricting the molecular movement of the polymer radicals through physical adsorption, pyrolysis was conducted in the presence of silica gel. The addition of silica gel powder accelerated the PS degradation, resulting in a drastic reduction in the molecular weight, but it increased the production of low molecular weight products, particularly the product with an M_n of 200. The significant increase in this M_n-200 product indicated that the product is formed through the direct decomposition of the PS, not through the cyclic trimer. The physical fluidity of the silica gel enhanced the molecular movement of the polymer chains, leading to the decomposition of the PS into the low-molecular weight products. On the other hand, less fluid molecular sieves accelerated the depolymerization during the PS degradation. Specifically, MS-4A molecular sieves increased the styrene yield to 66%. Increasing the pore size of the molecular sieves decreased the styrene yield but enhanced the toluene formation. The increase in toluene using larger pore size sieves indicated that toluene is generated at the polymer chain ends within the sieve pores. Given that the size of the PS chain end is 0.582 nm based on the bond lengths and angles (Fig. S3†), it is plausible to suggest that the toluene formation is accelerated within the larger pores of the MS-13X.

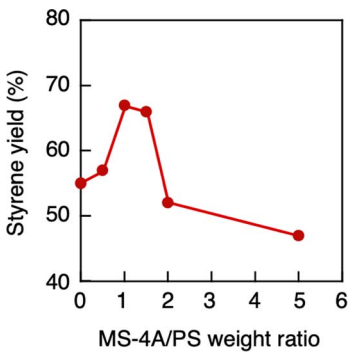

Fig. 11 Plots of the styrene yield *versus* the MS-4A/PS weight ratio for the pyrolysis by 20 min heating.

This study also investigated the relationship between the styrene yield and MS-4A weight ratio in order to further enhance styrene recovery. As shown in Fig. 11, the styrene reached its maximum at the MS-4A weight ratio of 1.0, then decreased beyond this ratio. Table 2 summarizes the area ratios of the products by 20 min pyrolysis for each MS-4A weight ratio. At the weight ratio of 1.0, MS-4A produced a 67% styrene yield without any detectable toluene. Increasing the MS-4A ratio to 1.5 resulted in a negligible change in the styrene yield, but promoted the PS degradation that formed the M_n-200 product and toluene. Further increasing the MS-4A ratio hindered the PS degradation, decreasing the styrene yield due to the strong adsorption of the chain ends on the sieves. However, compared to the non-additive pyrolysis producing a similar styrene yield, the excessive sieves at the 5.0 weight ratio effectively suppressed the backbiting and reduced the cyclic trimer formation. This suggested that stabilizing the polymer radicals through physical interaction is crucial for effectively advancing depolymerization.

Temperature effect

This study also investigated the effect of temperature on the pyrolysis process. The pyrolysis results by 20 min heating at different temperatures are shown in Fig. 12. Considering that the radical polymerization of styrene has a ceiling temperature of 310 °C,[52] no depolymerization occurred below this temperature. However, beyond this temperature, increasing the temperature led to an immediate rise in styrene yield through depolymerization. Notably, the temperatures above 400 °C facilitated the enhanced degradation of the PS, resulting in a rapid decrease in the molecular weight and PDI (Fig. 13). As depicted in Fig. 14, the PS degradation was further accelerated at 480 °C, but this degradation coincided with an increase in the M_n-200 product, despite negligible changes in the cyclic trimer and toluene. While the backbiting, the M_n-200 product is likely to result from random scission of the carbon–carbon backbone. At higher temperatures, the random scission of the main chain becomes more prevalent compared to the chain end reactions. Additionally, the pyrolysis at 480 °C necessitated heating along with flowing oxygen, resulting in partial deformation of the Pyrex tube. The pyrolysis at 420 °C or lower is more proper for conveniently recycling the PS foam waste.

Table 2 Effect of MS-4A on the vacuum pyrolysis depolymerization of the waste PS foam

				Area ratio (%)					
					M_n				
Weight ratio	St (%)	M_n	M_w/M_n	Polymer	950	500	300	200	Toluene (%)
—	55	17 500	1.90	45.5	3.9	1.5	43.0	6.1	2.2
0.5	57	24 800	2.76	29.0	5.8	2.7	54.1	8.4	1.2
1.0	67	20 300	2.20	37.8	4.6	2.8	48.5	6.3	0.0
1.5	66	17 900	2.15	24.1	4.2	2.5	46.4	22.8	6.0
2.0	52	26 400	3.15	37.1	3.9	2.6	45.3	11.2	2.4
5.0	47	16 500	2.14	73.0	0.0	0.6	18.7	7.8	4.9
—[a]	48	20 400	2.34	45.7	3.1	1.3	39.6	10.3	2.2

[a] Heating for 10 min.

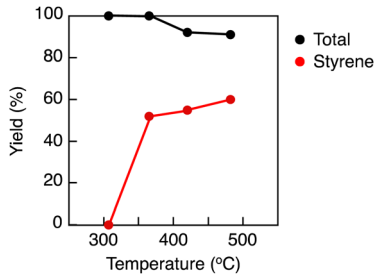

Fig. 12 Plots of the styrene and total yields *versus* temperature. Heating for 20 min.

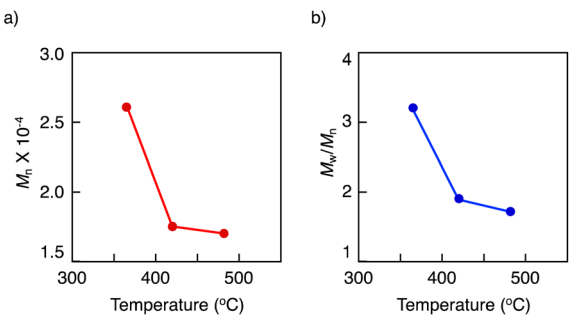

Fig. 13 Plots of (a) the molecular weight (M_n) and (b) PDI (M_w/M_n) of the residue *versus* temperature. Heating for 20 min.

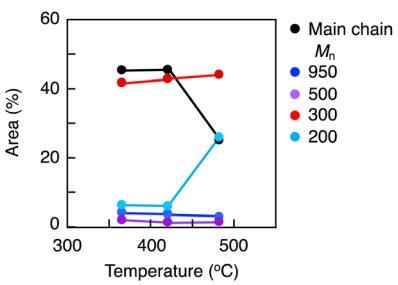

Fig. 14 Variations in area ratios of the decomposition products *versus* temperature.

Conclusions

This study provides a convenient chemical recycling method to recover high-purity styrene from waste PS foam by vacuum pyrolysis. The pyrolytic process involves a simple procedure of heating the PS foam using a spirit lamp for 20 min and collecting the monomer in a trap. The key to effectively recovering the monomer is to stabilize the chain end radicals, which helps suppress side reactions such as backbiting and radical coupling. This is achieved by physically adsorbing the chain radicals on the molecular sieves and increasing the temperature to improve the depolymerization process.

The distinctive feature of vacuum pyrolysis is its ability to perform depolymerization and fractionation simultaneously. This process produces gaseous pyrolysates and some aromatic compounds, such as dimers, trimers, and higher molecular weight oligomers, similar to other pyrolytic methods. However, a notable difference from these methods is that aromatic compounds with molecular weights higher than that of styrene do not move to a trap due to their high boiling points, even under reduced pressure, and thus remain in the reactor. Additionally, gaseous pyrolysates with low boiling points escape from the system. As a result, only styrene and a slight amount of toluene transfer to a trap as vapor under reduced pressure, ensuring a high-purity styrene recovery. This simple and convenient chemical recycling method does not require a special reactor or temperature controller, and it can be applied to other carbon–carbon backbone plastics. This method shows promise in reducing pollution caused by waste plastics. By returning waste plastics to their original fossil fuel state without the need for further fractionation and purification, it demonstrates that waste plastics are helpful as an alternative source for petroleum production, alongside crude oil, which is promising to reduce natural fossil fuel consumption.

Conflicts of interest

There are no conflicts to declare.

Acknowledgements

The author would like to thank Dr Ikuhide Fujisawa at Toyohashi University of Technology for his support in conducting the TOF-MS measurements.

References

1 D. Kwon, *Nature*, 2023, **616**, 234–237.
2 L. Lebreton and A. Andrady, *Palgrave Commun.*, 2019, **5**, 1–11.
3 R. Geyer, J. R. Jambeck and K. L. Law, *Sci. Adv.*, 2017, **3**, e1700782.
4 W. Zimmermann, *Philos. Trans. R. Soc., A*, 2020, **378**, 20190273.
5 C. M. Rochman, M. A. Browne, B. S. Halpern, B. T. Hentschel, E. Hoh, H. K. Karapanagioti, L. M. Rios-Mendoza, H. Takada, S. Teh and R. C. Thompson, *Nature*, 2013, **494**, 169–171.
6 R. M. Cywar, N. A. Rorrer, C. B. Hoyt, G. T. Beckham and E. Y.-X. Chen, *Nat. Rev. Mater.*, 2022, **7**, 83–103.
7 Z. Zhou, A. M. LaPointe, T. D. Shaffer and G. W. Coates, *Nat. Chem.*, 2023, **15**, 856–861.
8 W. B. Han, G.-J. Ko, K.-G. Lee, D. Kim, J. H. Lee, S. M. Yang, D.-J. Kim, J.-W. Shin, T.-M. Jang, S. Han, H. Zhou, H. Kang, J. H. Lim, K. Rajaram, H. Cheng, Y.-D. Park, S. H. Kim and S.-W. Hwang, *Nat. Commun.*, 2023, **14**, 2263.
9 S. Lambert and M. Wagner, *Chem. Soc. Rev.*, 2017, **46**, 6855–6871.
10 K. L. Law and R. Narayan, *Nat. Rev. Mater.*, 2022, **7**, 104–116.
11 A. Abdelhafidi, I. M. Babaghayou, S. F. Chabira and M. Sebaa, *Procedia Soc. Behav. Sci.*, 2015, **195**, 2922–2929.
12 A. L. Andrady, *Mar. Pollut. Bull.*, 2017, **119**, 12–22.
13 C. Avio, S. Gorbi and F. Regoli, *Mar. Environ. Res.*, 2017, **128**, 2–11.
14 M. Revel, A. Châtel and C. Mouneyrac, *Curr. Opin. Environ. Sci. Health*, 2018, **1**, 17–23.
15 W. Zhang, S. Zhang, J. Wang, Y. Wang, J. Mu, P. Wang, X. Lin and D. Ma, *Environ. Pollut.*, 2017, **231**, 541e548.
16 J. Hwang, D. Choi, S. Han, S. Y. Jung, J. Choi and J. Hong, *Sci. Rep.*, 2020, **10**, 7391.
17 K. Mattsson, E. V. Johnson, A. Malmendal, S. Linse, L.-A. Hansson and T. Cedervall, *Sci. Rep.*, 2017, **7**, 11452.
18 A. Rahimi and A. J. M. Garcia, *Nat. Rev. Chem.*, 2017, **1**, 0046.
19 D. M. K. W. Dissanayake, C. Jayasinghe and M. T. R. Jayasinghe, *Energy Build.*, 2017, **135**, 85–94.
20 P. Kershaw, A. Turra and F. Galgani, *Gesamp*, 2019, **https://repository.oceanbestpractices.org/bitstream/handle/11329/889/rs99e.pdf?sequence=1**.
21 Z. Huang, Q. Cui, X. Yang, F. Wang and X. Zhang, *J. Hazard. Mater.*, 2023, **446**, 130673.
22 J. Hidalgo-Crespo, C. M. Moreira, F. X. Jervis, M. Soto, J. L. Amaya and L. Banguera, *Energy Rep.*, 2022, **8**, 306–311.
23 K. S. Chun, N. M. Y. Fahamy, C. Y. Yeng, H. Choo, P. Ming M. and K. Y. Tshai, *J. Eng. Sci. Technol.*, 2018, **13**, 3445–3456.
24 T. A. Bayoumi and M. E. Tawfik, *Polym. Compos.*, 2017, **38**, 637–645.
25 H. Lu, D. J. Diaz, N. J. Czarnecki, C. Zhu, W. Kim, R. Shroff, D. J. Acosta, B. R. Alexander, H. O. Cole, Y. Zhang, N. A. Lynd, A. D. Ellington and H. S. Alper, *Nature*, 2022, **604**, 662–671.
26 P. Johar, E. L. Rylott, C. R. McElroy, A. S. Matharu and J. H. Clark, *Green Chem.*, 2021, **23**, 808–814.
27 P. Johar, E. L. Rylott, C. R. McElroy, A. S. Matharu and J. H. Clark, *RSC Sustain.*, 2023, **1**, 117–127.
28 Z. Huang, M. Shanmugam, Z. Liu, A. Brookfield, E. L. Bennett, R. Guan, D. E. V. Herrera, J. A. Lopez-Sanchez, A. G. Slater, E. J. L. McInnes, X. Qi and J. Xiao, *J. Am. Chem. Soc.*, 2022, **144**, 6532–6542.
29 G. Zhang, Z. Zhang and R. Zeng, *Chin. J. Chem.*, 2021, **39**, 3225–3230.
30 A. Pifer and A. Sen, *Angew. Chem., Int. Ed.*, 1998, **37**, 3306–3308.
31 S. E. Lewis, B. E. Wilhelmy Jr and F. A. Leibfarth, *Chem. Sci.*, 2019, **10**, 6270–6277.
32 R. Hasanzadeh, T. Azdast, M. Mojaver and C. B. Park, *Fuel*, 2022, **316**, 123362.
33 X. Liu, K. R. G. Burra, Z. Wang, J. Li, D. Che and A. K. Gupta, *J. Energy Resour. Technol.*, 2021, **143**, 052304.
34 A. M. Gonzalez-Aguilar, V. Pérez-García and J. M. Riesco-Ávila, *Polymers*, 2023, **15**, 1582.
35 H. M. Ng, N. M. Saidi, F. S. Omar, K. Ramesh and S. Bashir, *Encycl. Polym. Sci. Technol.*, 2018, 1–29.
36 I. M. Maafa, *Polymers*, 2021, **13**(225), 1–30.
37 C. Lu, H. Xiao and X. Chen, *e-Polym.*, 2021, **21**, 428–432.
38 Adnan, J. Shah and M. R. Jan, *J. Polym. Environ.*, 2017, **25**, 759–769.
39 X. Ren, Z. Huang, X.-J. Wang and G.-m. Guo, *J. Therm. Anal. Calorim.*, 2022, **147**, 1421–1437.
40 G. Albor, A. Mirkouei, A. G. McDonald, E. Struhs and F. Soto, *Processes*, 2023, **11**, 1126.
41 Z. Tamri, A. V. Yazdi, M. N. Haghighi, M. S. Abbas-Abadi and A. Heidarinasab, *Polyolefins J.*, 2019, **6**, 43–52.
42 N. M. Aljabri, Z. Lai, N. Hadjichristidis and K.-W. Huang, *J. Saudi Chem. Soc.*, 2017, **21**, 983–989.
43 R. Miandad, A. S. Nizami, M. A. Barakat, M. I. Khan, A. Mustafa, I. M. I. Ismail and J. D. Murphy, *Waste Manage.*, 2016, **58**, 250–259.
44 A. M. Gonzalez-Aguilar, V. P. Cabrera-Madera, J. R. Vera-Rozo and J. M. Riesco-Ávila, *Polymers*, 2022, **14**, 4957.
45 U.-S. Amjad, M. Ishaq, H. U. Rehman, N. Ahmad, L. Sherin, M. Hussain and M. Mustafa, *Environ. Prog. Sustainable Energy*, 2021, **40**, e13493.
46 M. Sogancioglu, E. Yel and G. Ahmetli, *Energy Procedia*, 2017, **118**, 189–194.
47 N. A. Abdullah, A. Novianti, I. I. Hakim, N. Putra and R. A. Koestoer, *IOP Conf. Ser. Earth Environ. Sci.*, 2018, **105**, 012033.
48 S. Fan, Y. Zhang, T. Liu, W. Fu and B. Li, *J. Anal. Appl. Pyrolysis*, 2022, **162**, 105425.
49 D. S. Achilias, I. Kanellopoulou, P. Megalokonomos, E. Antonakou and A. A. Lappas, *Macromol. Mater. Eng.*, 2007, **292**, 923–934.
50 A. Katsumiti, M. P. Losada-Carrillo, M. Barros and M. P. Cajaraville, *Sci. Rep.*, 2021, **11**, 22396.
51 C. Fuentes, J. C. Lerner, P. Vazquez and J. Sambeth, *Catal. Today*, 2021, **372**, 175–182.
52 G. Odian, *Principles of Polymerization*, John Wiley & Sons Inc., Hoboken, New Jersey, 4th edn, 2004.
53 D. E. Eastman, *Phys. Rev. B: Solid State*, 1970, **2**, 1.